Rock Mechanics and Rock Engineering (2021) 54:4347–4353
https://doi.org/10.1007/s00603-021-02482-3

TECHNICAL NOTE

Water-Weakening Effects on the Strength of Hard Rocks at Different Loading Rates: An Experimental Study

Jun Zhu[1] · Jianhui Deng[1] · Fei Chen[2,3] · Yuanjun Ma[1] · Yifan Yao[1]

Received: 17 August 2019 / Accepted: 19 April 2021 / Published online: 15 May 2021

Keywords Rock mechanics · Loading rate · Water-weakening effects · Uniaxial compression strength (UCS) · Dominant frequency

1 Introduction

Water is one of the most important environmental factors affecting rock mechanical properties, because most rock masses in engineering practice are in the moist or saturated state (Fig. 1). Previous studies have concluded that the uniaxial compressive strength (UCS) of rock is generally reduced to various degrees in the presence of water (Shakoor and Barefield 2009; Eunhye et al. 2017). Furthermore, several mechanisms related to water-weakening effects have been revealed through numerous experiments, including (a) clay mineral softening (Van Eeckhout 1976; Erguler and Ulusay 2009), (b) stress corrosion (Brantut et al. 2014), (c) pore water pressure (Atkinson 1984; Zhou et al. 2016; Huang et al. 2019), and (d) friction-weakening effects (Baud et al. 2000). Among them, clay mineral softening arises in rocks containing clay mineral (as its name implies), and stress corrosion often occurs in siliceous rocks (Atkinson et al. 1981; Masuda 2001). It should be noted that, the effects mentioned above are usually combined, and there is no generally accepted explanation due to the great differences in rock types as well as in loading conditions. Therefore, it is challenging to detangle the contribution of a specific mechanism and describe the extent of its effect.

The fracturing of engineering rock masses often occurs under varying loading rates. To date, many researchers have found increases in strength to various degrees as loading rate increases (rate-dependence), e.g., Lajtai et al. (1991), Li et al. (2017a) and Hou et al. (2019). Nevertheless, it is generally recognized that, pore water pressure becomes obvious for saturated rock from drained to undrained conditions with an increasing loading rate, implying great strength reduction (Obert and Duvall 1967; Zhou et al. 2018). Interestingly, there is a contradiction regarding the loading rate effects on strength for saturated rock. Hence, a comprehensive study is necessary to fill in the knowledge gaps concerning which effect is primary.

The acoustic emission (AE) technique and wave propagation can be used to analyze the real-time activities of microcracks and has, therefore, become an important analytical tool in rock mechanics (Ohnaka and Mogi 1982; Fan et al. 2013; Li et al. 2015a, b). Based on the first motion polarity method and the moment tensor method proposed by Zang et al. (1998) and Ohtsu et al. (1998), Li et al. (2017b) concluded by statistical analysis of AE dominant frequencies that the waveforms of low dominant frequency are produced by micro-tensile failure and waveforms of high dominant frequency are caused by micro-shear failure. Afterwards, the micro-failure mechanisms of marble under uniaxial compression, direct tension and flat loading Brazilian tension based on statistical analysis of AE dominant frequencies were studied by Zhang et al. (2018) and Wang et al. (2019). The abovementioned findings concerning the statistical analysis of AE dominant frequencies provide a new approach to investigate the rock failure process, which will be used in this study.

To eliminate the effects of clay mineral softening and stress corrosion, two rocks containing a single mineral and free of clay and siliceous minerals were selected for uniaxial

✉ Jianhui Deng
jhdeng@scu.edu.cn

[1] State Key Laboratory of Hydraulics and Mountain River Engineering, College of Water Resources and Hydropower, Sichuan University, Chengdu 610065, China

[2] College of Architecture and Civil Engineering, Chengdu University, Chengdu 610106, China

[3] College of Architecture and Environment, Sichuan University, Chengdu 610065, China

Fig. 1 Rock mass soaking in water, examples of bridge along the Jinsha River in Yunnan, China

compression tests. The UCS of dry and saturated rock samples under different loading rates was measured first. Then, an improved processing method was adopted to obtain the dominant frequencies of AE waveforms. On the basis of corresponding relation between the dominant frequencies of AE waveforms and micro-failure types, water-weakening effects on strength were revealed. The extent of dual effects on strength regarding loading rate was described qualitatively.

2 Experimental Procedure

2.1 Characteristics of Experimental Rocks

The samples were two Chinese rocks: marble from Baoxing, Sichuan Province, and limestone from Leibo, Sichuan Province. The mineral compositions of the two rocks were determined with the aid of X-ray diffractometer (XRD), noting that except for mineral, namely, calcite, there is no other secondary mineral. Excluding the effects of clay and siliceous minerals, rocks with a single mineral composition not only ensure homogeneity, but also provide a basis for the analysis of water-weakening effects on strength.

2.2 Sample Preparation

The marble and limestone specimens were cored and trimmed with the required dimensions of $\Phi 50 \times H100$ mm. Both ends of the samples were ground to achieve parallel, flat, and smooth surfaces to ensure a uniform load distribution. The physical and mechanical parameters of the two rock samples are listed in Table 1.

Forty marble specimens and 40 limestone specimens were finally prepared in this study. All samples were first dried in a 105 °C oven for 48 h. Each oven-dried sample was weighed after cooling to room temperature. Then, half of the samples were soaked in water for 8 h using the method of vacuum forced saturation and stood for 4 h, allowing water to fill the air-removed pores of the samples. As suggested by ASTM, the degree of the water saturation of dry and saturated specimens was measured by the atmospheric distillation method, and found its values were close to 0 and 1, respectively.

2.3 Experimental Equipment and Method

A rock mechanics test system (MTS815 Flex Test GT) with a maximum capacity of 1000 kN was used to conduct the UCS tests. The axial displacement was measured by a linear variable differential transformer (LVDT) and its measuring range was -2.5 to $+2.5$ mm. The loading rates were 0.01, 0.05, 0.1, 0.5, and 1 mm min^{-1} (approximately $1.67 \times 10^{-6} \sim 1.67 \times 10^{-4}$ s^{-1}).

AE signals released during the loading application were automatically captured using a three-dimensional real-time monitoring system (PCI-2). Eight micro30 sensors, which have a good frequency response and sensitivity, were installed symmetrically in the radial direction along the surface of the cylinder (Fig. 2). The sampling frequency was 1 MHz, and the pre-amplification was set as 40 dB.

Table 1 Physical and mechanical parameters of two rock samples

Rock type	Condition	Density, ρ_{dry} or ρ_{sat} (g cm^{-3})	P-wave velocity (m/s)	Porosity (%)	Water content (%)
Marble	Dry	2.64	4262	8.42	0
	Saturated	2.72	4581		3.01
Limestone	Dry	2.65	4409	5.25	0
	Saturated	2.70	4850		1.87

2.4 AE Waveform Data Processing

All AE waveforms recorded were processed into a single data file. With the aid of a MATLAB programming process, Fast Fourier transformation (FFT) was employed to obtain dominant frequency information efficiently. Figure 3 shows a typical AE waveform and its corresponding spectrum. The frequency corresponding to the greatest amplitude, namely, the normalized amplitude equal to 1 in the figure, is defined as the dominant frequency.

3 Experimental Results

3.1 Mechanical Results

Figure 4 shows the variation in the UCS of dry and saturated rocks under different loading rates. The UCS values increase with growing loading rates in both dry marble and limestone rocks. Unlike the findings reported by Goldsmith et al. (1976) and Olsson (1991), a markedly smaller increase in the average UCS is observed for dry rocks when higher loading rates (i.e., 0.5 and 1 mm min^{-1}) were approached.

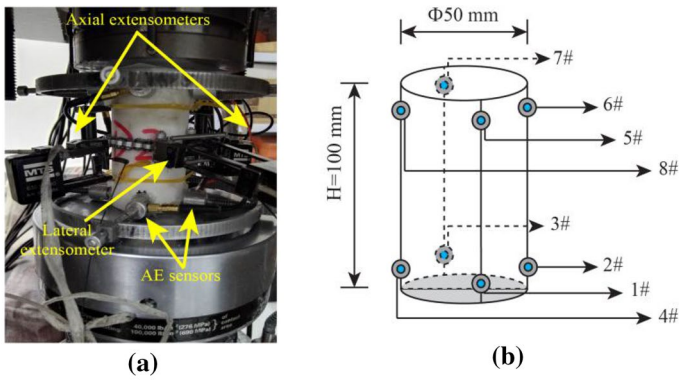

Fig. 2 Setup of uniaxial compressive test: **a** loading system and specimen with array of sensors before test, **b** schematic diagram of AE sensors layout

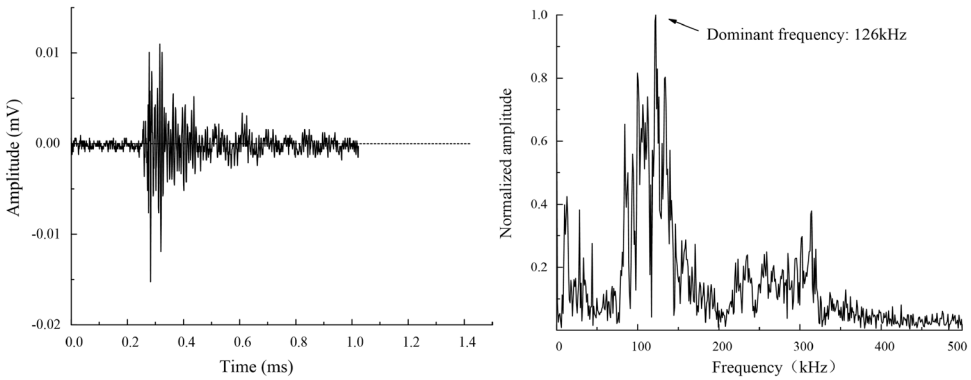

Fig. 3 Extraction process of dominant frequency through Fast Fourier transform (FFT)

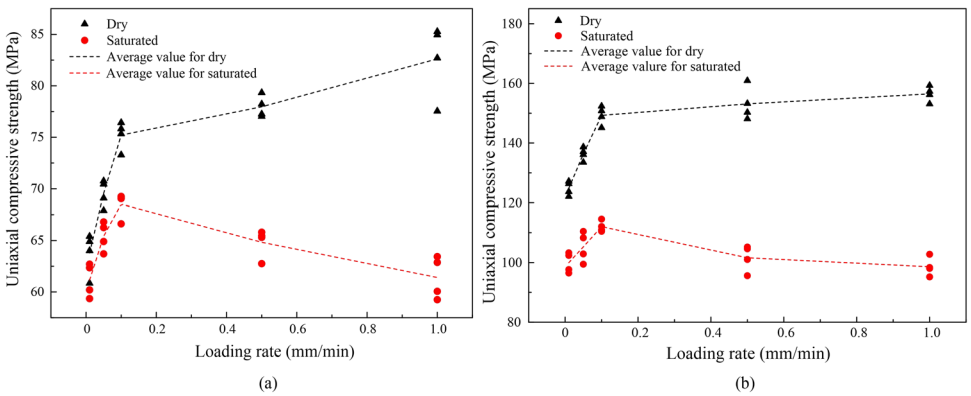

Fig. 4 Correlations of loading rate with uniaxial compressive strength (UCS) for two rocks: **a** dry and saturated marble, **b** dry and saturated limestone

A fascinating phenomenon interests us greatly in Fig. 4, that is, the UCS of the two saturated rocks increase, and then decrease with an increase in loading rates. When the loading rate varies from 0.01 to 0.1 mm min^{-1}, the UCS increases rapidly, while when the loading rate reaches 0.5 mm min^{-1} it decreases as the loading rate increases. Moreover, the UCS shows a decreasing trend at loading rate of 1 mm min^{-1} as well. This is possibly due to the variation of primary effect on UCS, which will be further analyzed in the discussion part. For simplicity, low loading rates consisting of 0.01, 0.05, and 0.1 mm min^{-1}, and high loading rates including 0.5 and 1 mm min^{-1} were defined in this study.

For both marble and limestone, the UCS decreases to various degrees after saturation. The softening coefficient is calculated by dividing the average UCS for saturated samples by that for dry samples. Compared to that of marble, the softening coefficient of limestone is significantly smaller, as shown in Fig. 5. This supports the conclusion that limestone has a stronger water-weakening effect on strength. In addition, the softening coefficient of both rocks reveals a negative correlation with loading rate, and the decrease at high loading rates seems less.

The elastic moduli of rock samples were determined with the average modulus of linear portion of axial stress–strain curve according to ASTM. In general, the elastic moduli for both rocks decrease after water adsorption, and are significantly correlated with variations in the loading rates (see Fig. 6). With an increase in loading rate, the elastic moduli increase relatively. Noticeably, the elastic moduli at high loading rates increase slightly, which is different from those at low loading rates.

3.2 Dominant Frequency Characteristics

As the dominant frequencies of AE waveforms in rock are mostly lower than 450 kHz, the dominant frequencies for each sample were classified into 46 bands to statistically analyze their characteristics. The first 45 bands include 0–450 kHz, and the range of each band is 10 kHz. Moreover, dominant frequencies higher than 450 kHz are divided into the No. 46 band. In line with the views of the research presented by Li et al. (2017b) and Huang et al. (2019), there are two concentrations of dominant frequency bands in all rock specimens, namely, the low dominant frequency band (L-type band) and the high dominant frequency band (H-type band). This further confirms that the characteristic of two-peak frequencies is intrinsic for rocks, regardless of loading rate.

As listed in Table 2, the average AE waveforms sum gradually decreases overall with increasing loading rates. The average AE waveforms sum of the two saturated rocks is far less than that of the dry rocks. The percentages of L-type bands in each sample at different loading rates are shown in Fig. 7. In particular, the UCS (160.93 MPa) and AE waveforms sum (8638) of rock sample 4-LD-3 show an obvious difference from those of others in the same group. Considering the differences among samples and

saturated limestone.

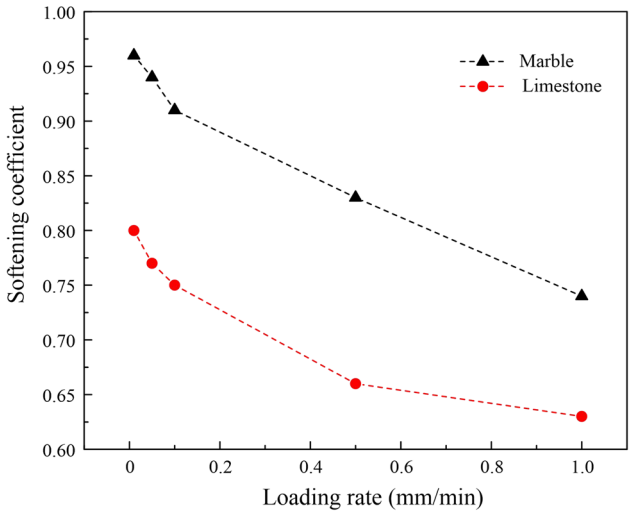

Fig. 5 Correlations of loading rate with softening coefficient for two rocks

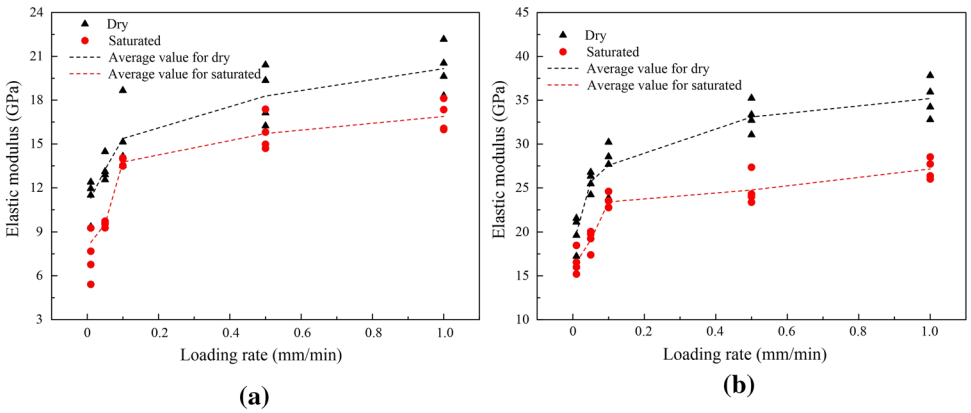

Fig. 6 Correlations of loading rate with elastic modulus for two rocks: **a** dry and saturated marble, **b** dry and saturated limestone

Table 2 Average percentages of H-type and L-type waveforms of two rock samples under different loading rates

Loading rates (mm min^{-1})	Rock condition	Marble			Limestone		
		Waveforms sum	Percentage of dominant frequency		Waveforms sum	Percentage of dominant frequency	
			H-type	L-type		H-type	L-type
0.01	Dry	74,123	65.88	29.52	107,569	64.97	31.05
	Saturated	62,469	17.40	78.41	86,820	24.78	73.29
0.05	Dry	68,838	69.47	26.35	79,232	66.98	28.76
	Saturated	55,618	22.38	73.15	64,697	27.42	69.50
0.1	Dry	39,561	72.55	22.65	62,907	70.26	23.91
	Saturated	36,550	28.75	68.74	43,859	29.65	65.45
0.5	Dry	17,783	75.16	21.25	25,707	65.41	29.44
	Saturated	17,860	14.07	80.74	19,600	21.37	75.75
1	Dry	2248	79.29	18.39	4460	75.81	19.85
	Saturated	881	12.59	85.36	1099	15.84	81.45

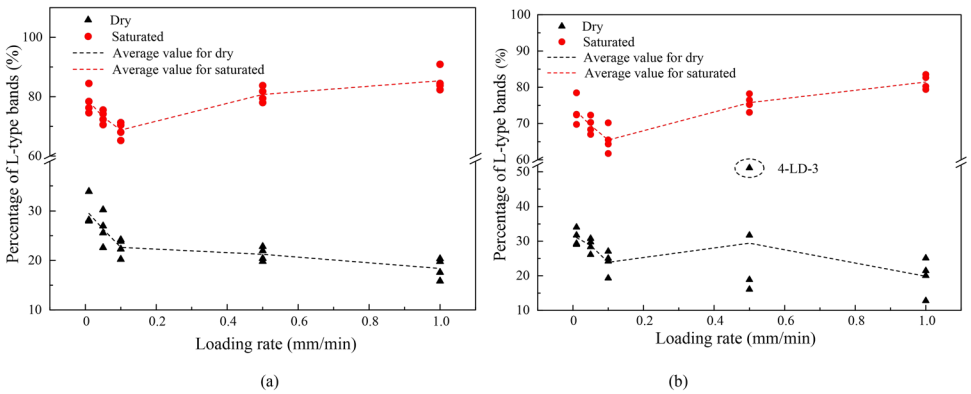

Fig. 7 Correlations of loading rates with percentages of L-type bands for two rocks: **a** dry and saturated marble, **b** dry and saturated limestone

the sensitivity of AE acquisition, the percentage of L-type waveforms for 4-LD-3, accounting for 51.11%, may not be consistent with the regularity of this group. In general, dry rocks are dominated by H-type AE signals, whereas saturated rocks are dominated by L-type AE signals. The percentages of L-type bands clearly increase after saturation, indicating that more micro-tensile failures are generated. The Percentage of L-type waveforms for saturated rocks relatively decreases at low loading rates, while it increases gradually at high loading rates. When the loading rate changed from 0.1 to 0.5 mm min^{-1}, the percentage of L-type bands for saturated marble on average increased from 68.74 to 80.74%, and this for saturated limestone range from 65.45 to 75.75%. For dry samples, excluding the result of 4-LD-3, the percentage of L-type bands gently decreased with an increase of loading rates. In addition, more dispersion was exhibited for dry limestone than that for dry marble.

4 Discussion

As the loading rate increases, the UCS for dry rocks gradually increases, while the UCS for saturated rocks rapidly increases at low loading rates, and then decreases at high loading rates. This phenomenon indicates that the positive correlation between UCS and loading rate changes due to the existence of water.

For dry rocks, the percentage of L-type waveforms decreases as the loading rate increases. Considering the corresponding relation between the dominant frequency bands of AE waveforms and micro failure types (Li et al. 2017b), it is evident that fewer micro-tensile failures, corresponding to L-type bands, are generated with increasing loading rates. Furthermore, the UCS of dry rocks is substantially, negatively correlated with the percentages of L-type bands, as shown in Fig. 8. It is well known that the ability of brittle rock to stretch is much lower than that to compress (Goodman 1989; Wu et al. 2018). Xie et al.

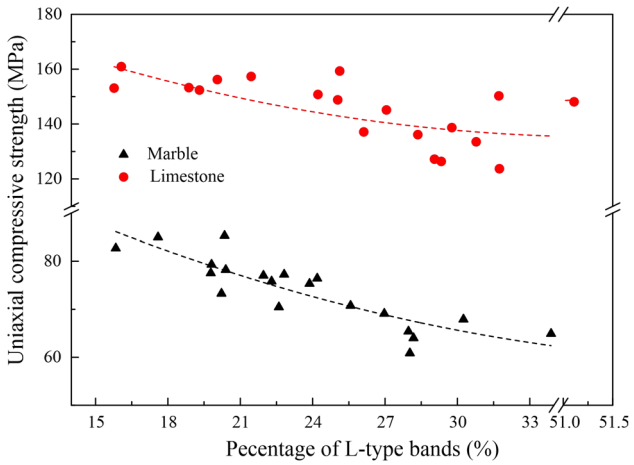

Fig. 8 Relationship between uniaxial compressive strength (UCS) and percentages of L-type bands for two rocks under dry condition

(2005) indicated that, the rock strength decreases as the degree of tension increases. In addition, Cai et al. (2007) reported that AE waveforms of low frequency correspond to large-scale fractures. These findings support the conclusion that the strength increase for dry rocks with an increasing loading rate mainly result from the fewer micro-tensile failures leading to large-scale fracture.

Since these two saturated rocks used in this study have specific mineral composition (calcite only), the pore water pressure is the main reason for strength reduction of saturated rocks (Huang et al. 2019; Zhu et al. 2020). As the loading rate increases, the micro-cracks propagate faster for saturated rocks so that water cannot reach the crack tips, thereby inducing greater pore water pressure. Furthermore, an increase in pore water pressure will decrease the effective pressure, which results in strength reduction (Li et al. 2016). Hence, the strength for saturated rocks is affected by two aspects, (1) strength increase due to the rate-dependence and (2) strength reduction resulting from pore water pressure. On the basis of the results for dry rocks, the percentage of L-type waveforms decreases due to the effect of (1). However, more micro-tensile failure generated by greater pore water pressure at higher loading rate will increase the percentage of L-type waveforms (Zhu et al. 2020). That is, (1) and (2) have opposite effects on the percentage of L-type waveforms. When loading rates increase within the range from 0.01 to 0.1 mm min^{-1}, effect (1) is dominant for the low pore water pressure. Fewer micro-tensile failures corresponding to low dominant frequencies of AE waveforms are generated, and the percentage of L-type waveforms decreases (see Fig. 7). The UCS of both two rocks increases with increasing loading rates because of the dominant effect of (1). However, as the loading rate increases within the high loading rate range, the pore water pressure resulting in micro-tensile failure becomes more obvious. In the presence of effect (1), effect (2) plays a dominant role and the percentage of L-type waveforms gradually increases shown in Fig. 7. Apparently, the more and more obvious pore water pressure is responsible for the decreasing UCS at high loading rates. In a word, the UCS of saturated rocks increases at low loading rates due to the primary role of rate-dependence, while the dominant effect of pore water pressure results in the decrease in the UCS at high loading rates.

To investigate the loading rate effects on strength for saturated rock from micro perspective, AE waveform analysis was adopted in this study. However, the higher the loading rate, the lower the AE waveforms sum, which may affect the reliability of statistical analysis. Further studies on the water-weakening effects of rock strength under various loading rates and determination of the critical loading rate are required.

5 Conclusions

Uniaxial compression tests at five loading rates (0.01, 0.05, 0.1, 0.5, and 1 mm min^{-1}) were performed on marble and limestone under dry and saturated conditions. Based on theoretical and experimental investigations, the following conclusions are drawn:

(1) As the loading rate increases, compared with the gradual increase in the UCS of dry rocks, the UCS of saturated rocks rapidly increases at low loading rates, and then decreases at high loading rates. The elastic moduli of two rocks increase slightly with growing loading rates.
(2) There are two concentrations of dominant frequency bands in both dry and saturated rocks. The percentage of L-type waveforms for dry rocks decreases relatively as the loading rate increases. At low loading rates, the percentage of L-type waveforms for saturated rocks relatively decreases, while it gently increases at high loading rates.
(3) With an increase of loading rate, fewer micro-tensile failures induced by rate-dependence result in an increase in the UCS of dry rocks. For saturated rocks, the decrease in UCS at low loading rates is responsible to the dominant effect of rate-dependence. However, the effect of enhanced pore water pressure leads to UCS reduction at high loading rates.

Acknowledgements This work was supported by the National Natural Science Foundation of China (Grant no. 41772322) and the National Key Research and Development Program of China (Grant no. 2018YFC1505004).

Declarations

Conflict of interest The authors declare that there is no conflict of interests regarding the publication of this article.

References

Atkinson BK (1984) Subcritical crack growth in geological materials. J Geophys Res Solid Earth 89(B6):4077–4114

Atkinson BK, Meredith PG (1981) Stress corrosion cracking of quartz: a note on the influence of chemical environment. Tectonophysics 77(1–2):T1–T11

Baud P, Zhu W, Wong TF (2000) Failure mode and weakening effect of water on sandstone. J Geophys Res Solid Earth 105(B7):16371–16389

Brantut N, Heap MJ, Baud P, Meredith PG (2014) Mechanisms of time-dependent deformation in porous limestone. J Geophys Res Solid Earth 119(7):5444–5463

Cai M, Kaiser PK, Morioka H, Minami M, Maejima T, Tasaka Y, Kurose H (2007) FLAC/PFC coupled numerical simulation of AE in large-scale underground excavations. Int J Rock Mech Min Sci 44(4):550–564

Erguler ZA, Ulusay R (2009) Water-induced variations in mechanical properties of clay-bearing rocks. Int J Rock Mech Min Sci 46(2):355–370

Eunhye K, Michael AS, Davi BM, Hossein C (2017) Correlations between the physical and mechanical properties of sandstones with changes of water content and loading rates. Int J Rock Mech Min Sci 100:255–262

Fan LF, Yi XW, Ma GW (2013) Numerical manifold method (nmm) simulation of stress wave propagation through fractured rock mass. Int J Appl Mech 05(2):1350022

Goldsmith W, Sackman JL, Ewerts C (1976) Static and dynamic fracture strength of Barre granite. Int J Rock Mech Min Sci Geomech Abst 13(11):303–309

Goodman RE (1989) Introduction to rock mechanics. Wiley, New York

Hou Z, Gutierrez M, Ma S, Almrabat A, Yang C (2019) Mechanical behavior of shale at different strain rates. Rock Mech Rock Eng 52:1–14

Huang YM, Deng JH, Zhu J (2019) An experimental investigation of moisture-induced softening mechanism of marble based on quantitative analysis of acoustic emission waveforms. Appl Sci 9(3):446

Lajtai EZ, Scott Duncan EJ, Carter BJ (1991) The effect of strain rate on rock strength. Rock Mech Rock Eng 24:99–109

Li JC, Li HB, Zhao J (2015a) An improved equivalent viscoelastic medium method for wave propagation across layered rock masses. Int J Rock Mech Min Sci 73:62–69

Li JC, Liu TT, Li HB, Liu YQ, Liu B, Xia X (2015b) Shear wave propagation across filled joints with the effect of interfacial shear strength. Rock Mech Rock Eng 48(4):1547–1557

Li Y, Chen YF, Zhou CB (2016) Effective stress principle for partially saturated rock fractures. Rock Mech Rock Eng 49(3):1091–1096

Li JC, Li NN, Li HB, Zhao J (2017a) An SHPB test study on wave propagation across rock masses with different contact area ratios of joint. Int J Impact Eng 105:109–116

Li LR, Deng JH, Zheng L, Liu JF (2017b) Dominant frequency characteristics of acoustic emissions in white marble during direct tensile tests. Rock Mech Rock Eng 50(5):1–10

Masuda K (2001) Effects of water on rock strength in a brittle regime. J Struct Geo 23:1653–1657

Obert L, Duvall WI (1967) Rock mechanics and the design of structures in rock. Wiley, New York

Ohnaka M, Mogi K (1982) Frequency characteristics of acoustic emission in rocks under uniaxial compression and its relation to the fracturing process to failure. J Geophys Res Solid Earth 87(B5):3873–3884

Ohtsu M, Okamoto T, Yuyama S (1998) Moment tensor analysis of acoustic emission for cracking mechanisms in concrete. ACI Struct J 95(2):87–95

Olsson WA (1991) The compressive strength of tuff as a function of strain rate from 10^{-6} to 10^{3}/sec. Int J Rock Mech Min Sci Geomech Abstr 28(1):115–118

Shakoor A, Barefield EH (2009) Relationship between unconfined compressive strength and degree of saturation for selected sandstones. Environ Eng Geosci 15(1):29–40

Van Eeckhout EM (1976) The mechanisms of strength reduction due to moisture in coal mine shales. Int J Rock Mech Min Sci Geomech Abstr 13(2):61–67

Wang YS, Deng JH, Li LR, Zhang ZH (2019) Micro-failure analysis of direct and flat loading Brazilian tensile tests. Rock Mech Rock Eng 52:4175–4187

Wu C, Chen X, Hong Y, Xu R, Yu D (2018) Experimental investigation of the tensile behavior of rock with fully grouted bolts by the direct tensile test. Rock Mech Rock Eng 51(1):351–357

Xie HP, Ju Y, Li LY (2005) Criteria for strength and structural failure of rocks based on energy dissipation and energy release principles. Chin J Rock Mechan Eng 24(17):3003–3010 (**in Chinese**)

Zang A, Wagner C, Stanchits F, Dresen S, Andresen GR, Haidekker MA (1998) Source analysis of acoustic emissions in Aue granite cores under symmetric and asymmetric compressive loads. Geophys J Int 135(3):1113–1130

Zhang ZH, Deng JH, Zhu JB, Li LR (2018) An experimental investigation of the failure mechanisms of jointed and intact marble under compression based on quantitative analysis of acoustic emission waveforms. Rock Mech Rock Eng 51(7):2299–2307

Zhou ZL, Cai X, Zhao Y, Chen L, Xiong C, Li XB (2016) Strength characteristics of dry and saturated rock at different strain rates. Trans Nonferrous Metals Soci Chin 26(7):1919–1925

Zhou ZL, Cai X, Ma D, Cao WZ, Chen L, Zhou J (2018) Effects of water content on fracture and mechanical behavior of sandstone with a low clay mineral content. Eng Fract Mech 193:47–65

Zhu J, Deng JH, Chen F, Huang YM, Yu ZQ (2020) Water saturation effects on mechanical and fracture behavior of marble. Int J Geomech. https://doi.org/10.1061/(ASCE)GM.1943-5622.0001825